LETTER

doi:10.1038/nature13451

The evolution of the placenta drives a shift in sexual selection in livebearing fish

B. J. A. Pollux[1,2], R. W. Meredith[1,3], M. S. Springer[1] & D. N. Reznick[1]

The evolution of the placenta from a non-placental ancestor causes a shift of maternal investment from pre- to post-fertilization, creating a venue for parent–offspring conflicts during pregnancy[1–4]. Theory predicts that the rise of these conflicts should drive a shift from a reliance on pre-copulatory female mate choice to polyandry in conjunction with post-zygotic mechanisms of sexual selection[2]. This hypothesis has not yet been empirically tested. Here we apply comparative methods to test a key prediction of this hypothesis, which is that the evolution of placentation is associated with reduced pre-copulatory female mate choice. We exploit a unique quality of the livebearing fish family Poeciliidae: placentas have repeatedly evolved or been lost, creating diversity among closely related lineages in the presence or absence of placentation[5,6]. We show that post-zygotic maternal provisioning by means of a placenta is associated with the absence of bright coloration, courtship behaviour and exaggerated ornamental display traits in males. Furthermore, we found that males of placental species have smaller bodies and longer genitalia, which facilitate sneak or coercive mating and, hence, circumvents female choice. Moreover, we demonstrate that post-zygotic maternal provisioning correlates with superfetation, a female reproductive adaptation that may result in polyandry through the formation of temporally overlapping, mixed-paternity litters. Our results suggest that the emergence of prenatal conflict during the evolution of the placenta correlates with a suite of phenotypic and behavioural male traits that is associated with a reduced reliance on pre-copulatory female mate choice.

Viviparity creates a venue for parent–offspring conflicts *in utero*[7] caused by a fundamental discord between mothers and developing embryos over the level of maternal investment during pregnancy. Females are selected to maximize their lifetime reproductive success by optimizing the allocation to each offspring while individual offspring are selected to demand a greater investment from the mother than is optimal for her to provide[1–4]. The ensuing evolutionary dynamics of perpetual adaptation and counter-adaptation between mother and developing embryo are hypothesized to be the driving force behind a rapid divergence in the genomic, developmental and physiological details of the placenta[1,3,6].

A central tenet of the parent–offspring conflict theory is that offspring must be able to manipulate the transfer of resources[1,7]. However, not all viviparous taxa have this capability[4–6]. Lecithotrophic viviparous species lack placentas and allocate all resources necessary for embryo development to the eggs before fertilization. This limits the potential for viviparity-driven conflict, because maternal investment pre-dates the expression of the paternal genome[1,2,4,6]. The evolution of the placenta from a non-placental lecithotrophic ancestor causes a shift in maternal investment from pre- to post-fertilization[5,6], offering embryos the opportunity to influence maternal investment throughout gestation[6,8,9]. This creates the potential for genomic conflicts, the magnitude of which depend on the extent of post-zygotic investment[1–4,6].

Theory predicts that the emergence of genomic conflicts, early in the evolution of the placenta, should drive a shift from a reliance on pre-copulatory mate choice to increasing levels of polyandry in conjunction with post-zygotic mechanisms of sexual selection[2]. Lecithotrophic species produce large, 'costly' (that is, fully provisioned) eggs[5,6], gaining most reproductive benefits by carefully selecting suitable mates based on phenotype or behaviour[2]. These females, however, run the risk of mating with genetically inferior (for example, closely related or dishonestly signalling) males, because genetically incompatible males are generally not discernable at the phenotypic level[10]. Placental females may reduce these risks by producing tiny, inexpensive eggs and creating large mixed-paternity litters by mating with multiple males. They may then rely on the expression of the paternal genomes to induce differential patterns of post-zygotic maternal investment among the embryos and, in extreme cases, divert resources from genetically defective (incompatible) to viable embryos[1–4,6,11].

Here we apply comparative methods to examine potential conflict-driven shifts in sexual selection associated with the evolution of post-fertilization maternal provisioning within the livebearing fish family Poeciliidae (order Cyprinodontiformes). This family presents a unique opportunity, because (1) it contains closely related species that differ markedly in the degree and timing of maternal provisioning, ranging from strict pre-zygotic yolk provisioning to extreme levels of post-zygotic investment associated with integrated maternal and fetal tissues specialized for nutrient transfer (that is, placentas[5,6]); (2) placentas were lost or evolved multiple times independently[5,6]; and (3) there is great interspecific variation in reproductive traits associated with pre-copulatory sexual selection, including caudal swords, enlarged dorsal fins and bright coloration in males[12–14]. Furthermore, a number of lineages have evolved the ability to carry multiple, temporally overlapping litters that are fertilized at different points in time (that is, superfetation[6,13,14]). In mammals, superfetation facilitates the formation of mixed-paternity litters (polyandry)[15–17]. Finally, molecular and experimental studies suggest that prenatal genomic conflicts occur in this family[18] and can result in differential patterns of post-zygotic maternal investment between developing embryos[19].

If substantial post-fertilization maternal provisioning intensifies fetal–maternal conflict[1,3] causing reduced female reliance on pre-copulatory cues in mate choice[2], then males of species with extensive post-fertilization maternal provisioning should display less developed, or the absence of, traits that facilitate female mate choice before copulation. Such traits include sexual dichromatism, courtship behaviour or ornaments. Moreover, if superfetation facilitates multiple paternity[15–17], then species with relatively high levels of post-fertilization provisioning should also have a higher probability of having superfetation[20,21]. Finally, copulation is known to incur costs to the females (for example, physical injury, reduced feeding opportunity, increased risk of predation and/or sexually transmitted diseases)[13,14]. If substantial post-fertilization maternal provisioning coincides with an increase in the frequency of polyandry, the ensuing sexual conflict should drive the evolution of female (resistance) traits that reduce the costs associated with superfluous mating attempts and, at the same time, male traits that enhance male mating success in the face of female resistance[14]. In Poeciliidae, a smaller male size relative to female size and an increase in gonopodium length (the male copulatory organ) increases the reproductive success of males

[1]Department of Biology, University of California, Riverside, California 92521, USA. [2]Experimental Zoology Group, Wageningen University, 6708 WD Wageningen, the Netherlands. [3]Department of Biology and Molecular Biology, Montclair State University, Montclair, New Jersey 07043, USA.

during sneaky or coercive copulation, which enables males to circumvent female choice[14,22–24]. We thus predict that males of species with a relatively higher post-zygotic maternal investment should display relatively smaller body sizes and longer gonopodia.

To test these hypotheses, we first quantified the degree of post-fertilization maternal provisioning for each species with the 'matrotrophy index', which is the estimated dry mass of the offspring at birth divided by the dry mass of the egg at fertilization. The matrotrophy index provides an objective, dimensionless measure of the degree of post-fertilization maternal provisioning that presents a proxy for the level of placentation[5,6]. Lecithotrophic species have matrotrophy index values of less than 1, because embryos lose dry mass during gestation[5,6]. Placentotrophic species have matrotrophy index values greater than 1, because post-fertilization maternal provisioning causes growth during development[5,6]. We employed a well-resolved phylogeny to test for predicted evolutionary shifts in sexual selection with Bayesian tests

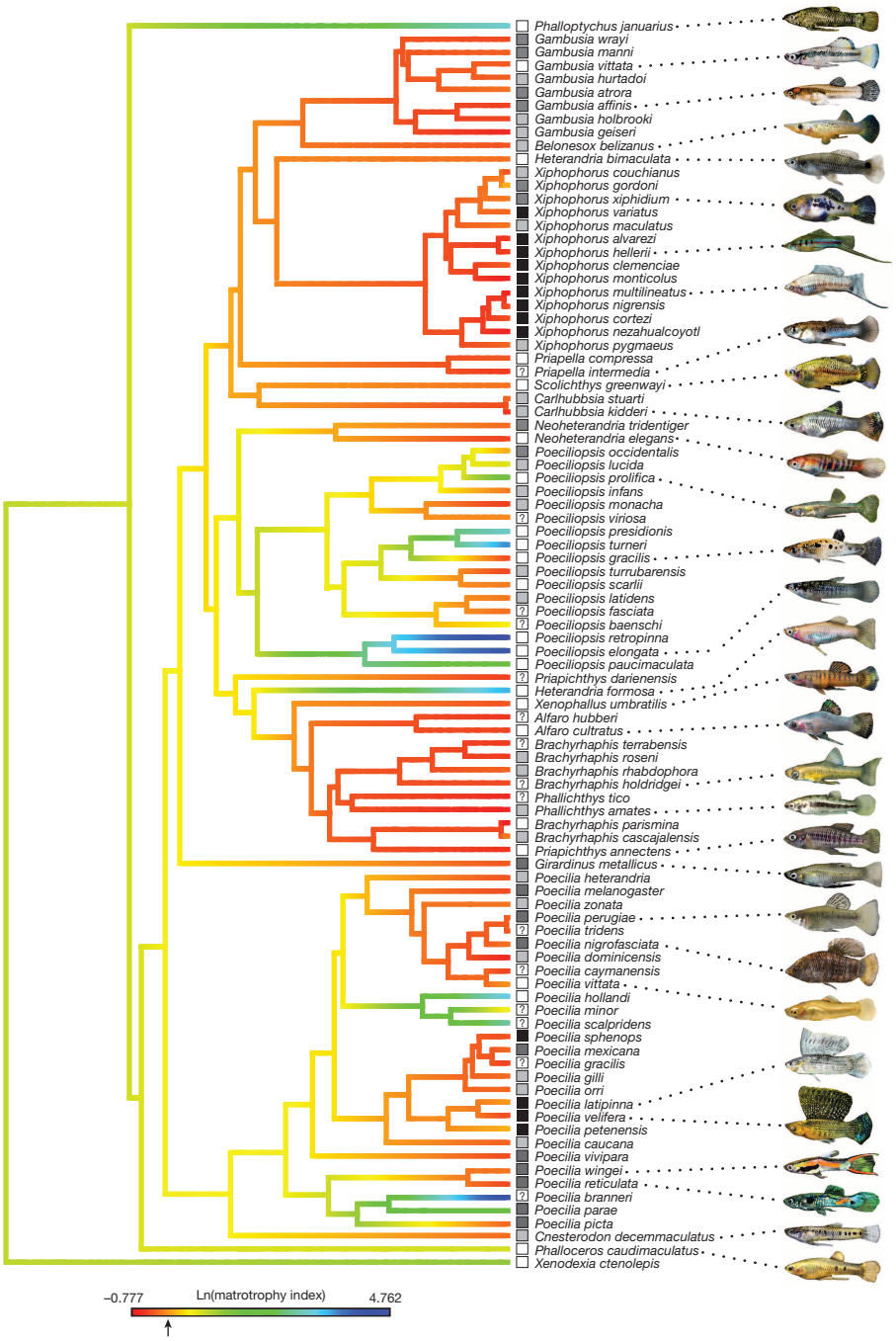

Figure 1 | Phylogenetic tree showing relationships among 94 species of the fish family Poeciliidae. Boxes at the terminal ends of the branches are coded according to the male sexual selection index: black = 3, dark grey = 2, light grey = 1 and white = 0; the boxed question mark indicates incomplete information (Supplementary Table 1). Branch colours depict a maximum likelihood reconstruction of maternal provisioning for log-transformed matrotrophy indices. The ancestral reconstruction was performed with phytools[30] and a Brownian motion model of trait evolution. The arrow on the scale bar corresponds to a matrotrophy index value of 1.0, which indicates the division between lecithotrophic and placentotrophic species. In agreement with previous analyses[5,6], the ancestral reconstruction suggests a complex history for the evolution of placentotrophy. The current analysis suggests that the common ancestor of the family has a placenta and that there were multiple losses and gains of placentation within the family. A caveat is that the single egg-layer within Poeciliidae (*Tomeurus gracilis*) was excluded from the analysis. The inclusion of this taxon, along with outgroups that contain both livebearers and egg-layers, may yield different results for the evolutionary history of placentotrophy within Poeciliidae.

of correlated trait evolution and phylogenetic linear and logistic regressions that explain the variation in sexually selected traits as a function of matrotrophy index (Fig. 1).

Bayesian tests show that matrotrophy index, and sexually dimorphic coloration (dichromatism) and courtship behaviour, respectively, have evolved in a correlated fashion (log(Bayes factor) = 13.308 and 3.438, respectively). Phylogenetic logistic regressions further show that both traits are negatively correlated to matrotrophy index ($b_1 = -0.614$, $P = 0.007$ and $b_1 = -0.763$, $P = 0.007$, respectively), indicating that these are significantly less likely to be found in placental lineages (Fig. 2a, b). The presence of exaggerated male display traits (that is, enlarged dorsal fins and filamentous extensions on upper maxillae in the genus *Poecilia* or extension of ventral part of the caudal fin to form a sword in *Xiphophorus*) is also negatively correlated with matrotrophy index, but this trend is not significant after correcting for phylogeny ($b_1 = -0.413$, $P = 0.429$; log(Bayes factor) = 0.663; Fig. 2c). The sexual selection index, defined as the summed presence of these three male traits (dichromatism, courtship behaviour and ornamental display traits), decreases significantly with increasing matrotrophy index (phylogenetic generalized least-squares regression: $F_{77} = 5.836$, $P = 0.018$; log(Bayes factor) = 2.320), indicating that lecithotrophic males have significantly more traits to facilitate female choice before copulation than highly placental species (Fig. 2d).

Superfetation is strongly correlated with matrotrophy index (phylogenetic logistic regression: $b_1 = 0.776$, $P < 0.001$; log(Bayes factor) = 25.730; Fig. 2e), indicating that placental species are more likely to have it. The relative length of the gonopodium is positively correlated with matrotrophy index (phylogenetic generalized least-squares regression: $F_{89} = 6.379$, $P = 0.013$; log(Bayes factor) = 4.214; Fig. 2f), demonstrating a strong association between longer genitalia and the presence of post-fertilization maternal provisioning. The size dimorphism index is also positively correlated with matrotrophy index, both for body weight ($F_{76} = 18.869$, $P < 0.001$; log(Bayes factor) = 6.664; Fig. 2g) and standard length ($F_{87} = 29.753$, $P < 0.001$; log(Bayes factor) = 4.948; Fig. 2h), indicating that the difference in body size between males and females is larger in lineages with higher levels of post-zygotic maternal investment. This increase is caused by a decrease in male size ($\log_{10}$(male wet mass): $F_{81} = 3.493$, $P = 0.065$, log(Bayes factor) = 3.676; $\log_{10}$(male standard length): $F_{89} = 2.022$, $P = 0.158$, log(Bayes factor) = 1.310; Fig. 2i, j blue lines) in association with increasing matrotrophy index, rather than an increase in female size ($\log_{10}$(female wet mass): $F_{76} = 0.021$, $P = 0.886$. log(Bayes factor) = 0.122; $\log_{10}$(female standard length): $F_{87} = 0.002$, $P = 0.962$, log(Bayes factor) = 0.298; Fig. 2i, j red lines).

Our findings yield three important insights. First, male traits that facilitate pre-copulatory female mate choice are less well developed in placental lineages. This is supported by patterns within individual clades. In the northern clade of the genus *Poeciliopsis*[5], males from lecithotrophic species are melanic whereas males from derived placental species have the same coloration as females. In the subgenus *Micropoecilia* of *Poecilia*, males belonging to the lecithotrophic clade are far more intensely coloured than the males in the derived placental clade, suggesting that here too sexually dimorphic coloration is disappearing. Extreme male ornamental display traits used during courtship are only found in lecithotrophic clades (*Xiphophorus* and subgenus *Mollienesia* of *Poecilia*) and are notably absent in placental species. Since sexual selection in Poeciliidae is influenced by pre-copulatory cues[12–14], these results suggest that phenotype- or behaviourally based female mate choice is of greater importance in lecithotrophic species than in species with substantial post-zygotic maternal provisioning.

Second, male traits that help circumvent female mate choice during sneak or coercive mating are more developed in placental species. These findings concur with the theory that sexual conflict can result in the evolution of sexual dimorphism[25,26] and rapid phenotypic divergence in genitalia[27,28]. In poeciliids, large males and short genitals are associated with courtship behaviour aimed at attracting cooperative females[12–14]. Smaller males and longer genitalia are associated with sneak copulation,

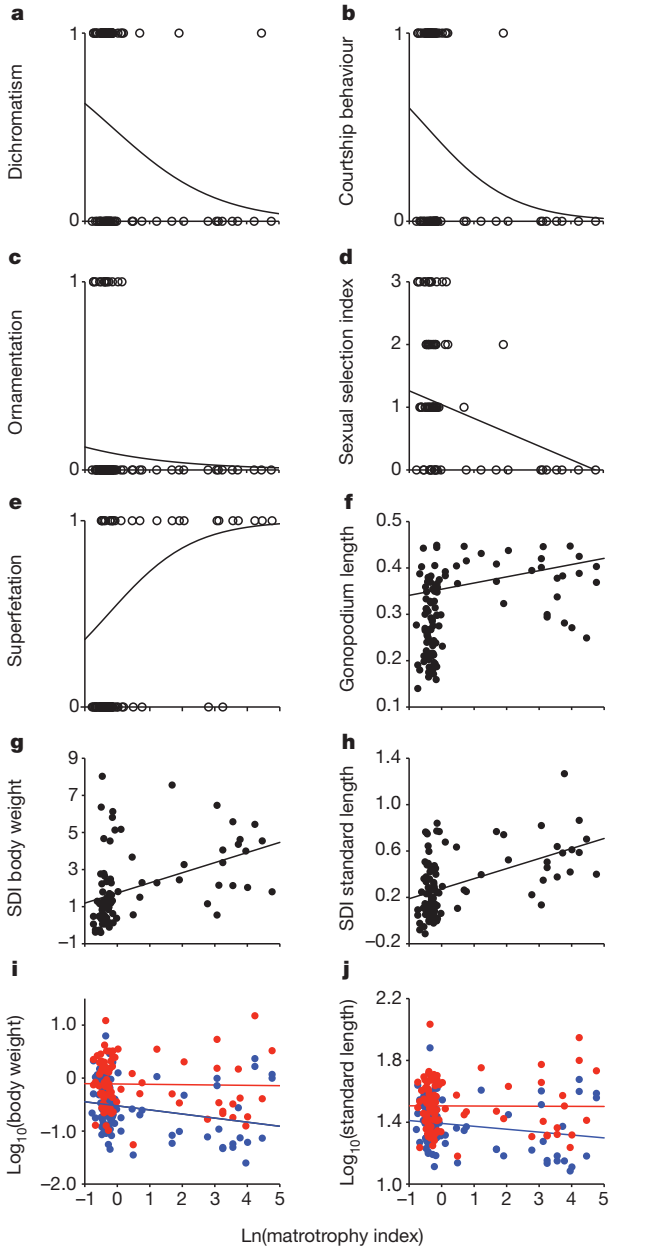

Figure 2 | Phylogenetic logistic and linear regressions. The regressions evaluate the effect of the natural-log-transformed matrotrophy index on (**a**) dichromatism ($n = 94$ taxa), (**b**) courtship behaviour ($n = 79$), (**c**) ornamental male display traits ($n = 94$), (**d**) sexual selection index (defined as the total number of male traits present ranging from 0 (none of the three traits present) to maximum 3 (all three traits present); $n = 79$), (**e**) superfetation ($n = 92$), (**f**) relative gonopodium length ($n = 107$ taxa), (**g**) size dimorphism index (SDI) for body weight ($n = 87$), (**h**) size dimorphism index for standard length ($n = 100$), (**i**) $\log_{10}$-transformed male (blue dots and line, $n = 99$) and female (red dots and line, $n = 87$) body weight, and (**j**) $\log_{10}$-transformed male (blue dots and line, $n = 107$) and female (red dots and line, $n = 100$) standard length.

the small size allowing males to approach females from behind without being detected and enabling them to manoeuvre more easily when inserting the gonopodium into the gonoduct of uncooperative females, while longer gonopodia enable a more efficient sperm transfer during unsolicited matings[12–14,22–24].

Third, the degree of post-zygotic maternal provisioning is strongly correlated with superfetation, which is found in all placental lineages save for *Phalloceros caudimaculatus* and the subgenus *Pamphorichthys* of *Poecilia*. This reproductive adaptation is thought to diminish the

probability of a single male monopolizing an entire litter by fertilizing all embryos. Instead, by dividing offspring into multiple, smaller temporally overlapping litters, each fertilized at different points in time, and by using sperm derived from the most recent mating event ('last male sperm precedence'[13,14]), superfetation increases a female's likelihood of creating multiple-paternity litters[15–17].

Prior research has shown that male coloration, courtship behaviour and ornamental display traits play an important role in pre-copulatory female mate choice[13–14], that small male size and long genitalia facilitate sneak copulation (a strategy that circumvents female choice)[13,14,22–24] and that superfetation facilitates the formation of mixed-paternity litters (polyandry)[15–17]. The correlation of these traits with the level of post-zygotic maternal provisioning provides support for an association between the placenta and weaker pre-copulatory mate choice. What remains to be shown is that this relationship is causal and is associated with an increase in multiple paternities. Our study provides the first empirical evidence concurring with the hypothesis[2] that the rise of parent–offspring conflicts during the evolutionary transition from pre- to post-zygotic maternal provisioning correlates with a shift in sexual selection. This study will help to understand the elusive consequences of viviparity-driven conflict and may advance our knowledge about the evolution of reproductive traits in other viviparous lineages that evolved placentas, since all share the same potential for genomic conflict.

METHODS SUMMARY

The maximum likelihood phylogeny was constructed using RAxML 7.0.4 (ref. 29). Different phylogenetic comparative approaches were used to test for correlated trait evolution.

Online Content Methods, along with any additional Extended Data display items and Source Data, are available in the online version of the paper; references unique to these sections appear only in the online paper.

Received 12 August 2013; accepted 2 May 2014.
Published online 9 July 2014.

1. Haig, D. Genetic conflicts in human pregnancy. *Q. Rev. Biol.* **68,** 495–532 (1993).
2. Zeh, D. W. & Zeh, J. A. Reproductive mode and speciation: the viviparity-driven conflict hypothesis. *Bioessays* **22,** 938–946 (2000).
3. Wilkins, J. R. & Haig, D. What good is genomic imprinting: the function of parent-specific gene expression. *Nature Rev. Genet.* **4,** 359–368 (2003).
4. Crespi, B. & Semeniuk, C. Parent-offspring conflict in the evolution of vertebrate reproductive mode. *Am. Nat.* **163,** 635–653 (2004).
5. Reznick, D. N., Mateos, M. & Springer, M. S. Independent origins and rapid evolution of the placenta in the fish genus *Poeciliopsis*. *Science* **298,** 1018–1020 (2002).
6. Pollux, B. J. A., Pires, M. N., Banet, A. I. & Reznick, D. N. The evolution of placentas in the fish family Poeciliidae – an empirical study of macroevolution. *Annu. Rev. Ecol. Evol. Syst.* **40,** 271–289 (2009).
7. Trivers, R. L. Parent-offspring conflict. *Am. Zool.* **14,** 249–264 (1974).
8. Banet, A. I., Au, A. G. & Reznick, D. N. Is mom in charge? Implications of resource provisioning on the evolution of the placenta. *Evolution* **64,** 3172–3182 (2010).
9. Pollux, B. J. A. & Reznick, D. N. Matrotrophy limits a female's ability to adaptively adjust offspring size and fecundity in fluctuating environments. *Funct. Ecol.* **25,** 747–756 (2011).
10. Zeh, J. A. & Zeh, D. W. Toward a new sexual selection paradigm: polyandry, conflict and incompatibility. *Ethology* **109,** 929–950 (2003).
11. Haig, D. Brood reduction and optimal parental investment when offspring differ in quality. *Am. Nat.* **136,** 550–556 (1990).
12. Bisazza, A. Male competition, female mate choice and sexual size dimorphism in poeciliid fishes. *Mar. Behav. Physiol.* **23,** 257–286 (1993).
13. Meffe, G. K. & Snelson, F. F. Jr. (eds). *Ecology and Evolution of Livebearing Fishes (Poeciliidae)* (Prentice Hall, 1989).
14. Evans, J. P., Pilastro, A. & Schlupp, I. (eds) *Ecology and Evolution of Poeciliid Fishes* (Univ. Chicago Press, 2011).
15. Shackelford, R. M. Superfetation in the ranch mink. *Am. Nat.* **86,** 311–319 (1952).
16. Yamaguchi, N., Dugdale, H. L. & MacDonald, D. W. Female receptivity, embryonic diapause, and superfetation in the European badger (*Meles meles*): implications for the reproductive tactics of males and females. *Q. Rev. Biol.* **81,** 34–48 (2006).
17. Dugdale, H. L., MacDonald, D. W., Pope, L. C. & Burke, T. Polygynandry, extra-group paternity and multiple-paternity litters in European badger (*Meles meles*) social groups. *Mol. Ecol.* **16,** 5294–5306 (2007).
18. O'Neill, M. J. *et al.* Ancient and continuing Darwinian selection on insulin-like growth factor II in placental fishes. *Proc. Natl Acad. Sci. USA* **104,** 12404–12409 (2007).
19. Schrader, M. & Travis, J. Testing the viviparity-driven-conflict hypothesis: parent-offspring conflict and the evolution of reproductive isolation in a poeciliid fish. *Am. Nat.* **172,** 806–817 (2008).
20. Coleman, S. W., Harlin-Cognato, A. & Jones, A. G. Reproductive isolation, reproductive mode, and sexual selection: Empirical tests of the viviparity-driven conflict hypothesis. *Am. Nat.* **173,** 291–303 (2009).
21. Schrader, M. & Travis, J. Variation in offspring size with birth order in placental fish: A role for asymmetric sibling competition? *Evolution* **66,** 272–279 (2012).
22. Bisazza, A. & Marin, G. Sexual selection and sexual size dimorphism in the eastern mosquitofish *Gambusia holbrooki* (Pisces Poeciliidae). *Ethol. Ecol. Evol.* **7,** 169–183 (1995).
23. Pilastro, A., Giacomello, E. & Bisazza, A. Sexual selection for small size in male mosquitofish (*Gambusia holbrooki*). *Proc. R. Soc. Lond. B* **264,** 1125–1129 (1997).
24. Evans, J. P. *et al.* Intraspecific evidence from guppies for correlated patterns of male and female genital trait diversification. *Proc. R. Soc. B* **278,** 2611–2620 (2011).
25. Arnqvist, G. & Rowe, L. Antagonistic coevolution between the sexes in a group of insects. *Nature* **415,** 787–789 (2002).
26. Bonduriansky, R. & Chenoweth, S. F. Intralocus sexual conflict. *Trends Ecol. Evol.* **24,** 280–288 (2009).
27. Arnqvist, G. Comparative evidence for the evolution of genitalia by sexual selection. *Nature* **393,** 784–786 (1998).
28. Hosken, D. J. & Stockley, P. Sexual selection and genital evolution. *Trends Ecol. Evol.* **19,** 88–93 (2004).
29. Stamatakis, A. RAxML-VI-HPC: maximum likelihood-based phylogenetic analyses with thousands of taxa and mixed models. *Bioinformatics* **22,** 2688–2690 (2006).
30. Revell, L. J. phytools: an R package for phylogenetic comparative biology (and other things). *Methods Ecol. Evol.* **3,** 217–223 (2012).

Supplementary Information is available in the online version of the paper.

Acknowledgements We thank all individuals and institutions who provided samples for this study (Rehoboth Aquatics, H. Bart Jr, R. Davis, D. Fromm, J. de Greef, H. Hieronimus, B. Hobbs, T. Hrbek, J. Johnson, B. Kohler, J. Langenhammer, C. Li, J. Lundberg, M. Mateos, A. Meyer, D. Nelson, L. Page, L. Parenti, M. Sabaj Pérez, R. Robins, R. de Ruiter, S. Schaefer, M. Schartl, J. Sparks, M. Stiassny, J. Travis, J. Trexler and J. Williams); L. Rowe and A. Furness for discussions and reading the manuscript; C. Oufiero and M. Banet for help in collecting part of the data; and T. Garland Jr for providing some of the phylogenetic statistical packages. This study was supported by Rubicon grant 825.07.017 of the Netherlands Organisation for Scientific Research and Marie Curie – IIF grant 299048 of the European Union to B.J.A.P. and grant DEB0416085 of the US National Science Foundation to D.N.R. and M.S.S.

Author Contributions B.J.A.P. and D.N.R. designed the study, D.N.R. quantified the matrotrophy indices, R.W.M. and M.S.S. constructed the molecular phylogeny, and B.J.A.P. measured the morphological traits, analysed the data and wrote the paper. All authors discussed the results and commented on the manuscript.

Author Information Reprints and permissions information is available at www.nature.com/reprints. The authors declare no competing financial interests. Readers are welcome to comment on the online version of the paper. Correspondence and requests for materials should be addressed to B.J.A.P. (b.pollux@gmail.com; bart.pollux@wur.nl) or D.N.R. (david.reznick@ucr.edu).

METHODS

Matrotrophy index. The degree of pre- versus post-fertilization maternal provisioning was estimated for 110 species of the family Poeciliidae by calculating the matrotrophy index, which is defined as the ratio of the estimated dry mass of the offspring at birth divided by the dry mass of the egg at fertilization. The stage of embryo development was assigned on the basis of morphological criteria[5] and converted into a numerical score that ranged from 0 (yolked egg, no development) to 45 (fully developed embryo, ready to be born), with stage 50 representing a newborn young. The numerator and denominator were estimated from a regression line fitted to the log-transformed dry masses of embryos (y axis) and their stage of development (x axis). The matrotrophy index provides an objective dimensionless measure of the degree of post-fertilization maternal provisioning that can be used as a proxy for the level of placentation[5]. Lecithotrophic species have matrotrophy index values ranging from 0.5 to 0.75, meaning that the embryos lose 25–50% of their dry mass during gestation due to metabolic costs associated with development; similar mass losses are observed in egg-laying species of fish[5]. Placentotrophic species have matrotrophy index values that range from near 1, implying some post-fertilization provisioning to offset the costs of development, to more than 100, indicating extensive post-fertilization maternal provisioning.

Sexually selected traits and superfetation. We obtained information on superfetation and the presence of sexually dimorphic coloration (dichromatism), courtship behaviour and exaggerated display traits in males from the literature and personal observations (all data are provided in Supplementary Table 1). Observed species were monitored twice for 20 min at room temperature in 37.8 l stock tanks containing gravel, aquatic plants and artificial lighting. We calculated a pre-copulatory sexual selection index for each species by assigning a value of 1 to each of the three male traits if they were present and then taking the sum. The sexual selection index indicated the total number of these traits present in the males of each species and ranged from 0 (indicating an absence of these male traits) to maximum 3 (indicating the presence of all three traits).

Morphological measurements. Information on sexual size dimorphism and genital length was obtained from preserved specimens (all data are provided in Supplementary Table 2). Standard length of preserved specimens was measured (to the nearest 0.01 mm) from the tip of the upper jaw to the outer margin of the hypural plate, using digital callipers. Gonopodium length was taken as the distance between the base of the gonopodium and its distal tip. The gonopodium is the male's copulatory organ derived from a metamorphosed anal fin and used to transfer sperm bundles (spermatozeugmata) into the female's urogenital opening. Relative gonopodium length was calculated as the ratio of gonopodium length to male standard length. The wet mass was measured to the nearest 0.01 mg on a Mettler AE 163 Microbalance (Mettler Instruments) after removal of excess liquid. Sexual size dimorphism (for body weight and standard length) was quantified as (1) the log of size ratio between females and males (sexual size dimorphism = log(female size/male size)) and (2) the size dimorphism index, which takes the ratio of the larger to the smaller sex and then subtracts 1 (size dimorphism index = (larger sex/smaller sex) − 1). This latter value is made negative if males are the larger sex and positive if females are the larger sex[31,32]. For all statistical analyses, body weight and standard length were $\log_{10}$ transformed.

Molecular sequences and phylogeny reconstruction. We assembled a data set that consisted of segments from 28 different genes (20 nuclear, 8 mitochondrial). Sequences were extracted from GenBank and supplemented with 920 new sequences for seven nuclear genes (*ENC1*, *Glyt*, *SH3PX3*, *MYH6*, *Rag1*, *Rh*, *X-src*) and two mitochondrial genes (*Cytb*, *ND2*). The data set comprised sequences for 288 species (293 terminals) of clupeocephalans of which 177 were poeciliids. Taxon sampling and GenBank accession numbers are provided in Supplementary Table 3. Tissue/DNA samples for this project were provided to D.N.R. by different individuals/institutions (see Acknowledgements) and are now housed at the University of California Riverside. Genomic DNA was extracted from either whole fish or fin clips using AccuPrep Genomic DNA Extraction Kits (Bioneer). Some samples proved difficult to amplify. In these cases we used Illustra GenomiPhi V2 DNA Amplification Kits (GE Healthcare) to amplify whole genomic DNA before PCR. Two mitochondrial and seven nuclear gene regions were targeted in PCR reactions. Mitochondrial DNA amplicons were as follows: (1) 3′ end of $tRNA^{Glu}$, complete cytochrome *b* (*cytb*), and 5′ end of $tRNA^{Thr}$; and (2) 3′ end of $tRNA^{Gln}$, complete $tRNA^{Met}$, complete NADH dehydrogenase subunit 2 (ND2), complete $tRNA^{Trp}$, complete $tRNA^{Ala}$, and 5′ end of $tRNA^{Asn}$. Nuclear amplicons were as follows: (1) two partial exons (8 and 10), all of exon 9, and two introns (8 and 9) of the tyrosine kinase gene (*X-src*); (2) exon 1 of myosin, heavy polypeptide 6 (*MYH6*); (3) exon 2 of ectodermal-neural cortex 1 like protein (*ENC1*); (4) exon 2 of glycosyltransferase (*Glyt*); (5) exon 1 of SH3 and PX domain containing 3 (*SH3PX3*); (6) a portion of the 7 transmembrane receptor region of rhodopsin (*Rh*); and (7) exon 3 of recombination activating gene-1 (*Rag1*). The majority of primers used have previously been described: *X-src* (refs 33–35); *MYH6*, *ENC1*, *Glyt*, *SH3PX3* (refs 34–36); *Rh* (refs 34, 35, 37); *Rag1*, *ND2* (refs 34, 35, 38–41); *cytb* (refs 34, 35, 42). Additional primers new to this study were designed as necessary. All primers used in this study can be found in Supplementary Table 4. PCR reactions, including nested PCRs, were performed following protocols outlined in refs 34, 35. All PCR products were run out on 1% agarose gels and the product of interest was excised and cleaned using AccuPrep Gel Purification kits (Bioneer). Cleaned PCR products were sequenced in both directions using an automated DNA sequencer (ABI 3730xl) at the University of California Riverside's Core Genetics Institute. Sequencher 4.8 was used to assemble contigs. All sequences were manually aligned in Se-Al[43]. Alignment ambiguous regions, including several transfer RNA (tRNAs) (Gln, Met, Trp, Ala, Asn), were visually identified and removed before performing phylogenetic analyses. The final DNA alignment for the 28 gene segments without alignment ambiguous regions was 20,828 base pairs. We divided the concatenated data set into 22 partitions. The mitochondrial gene regions were partitioned into protein-coding genes and RNAs (tRNA, ribosomal RNA) and each nuclear gene region was given its own partition. jModelTest was used to determine the best-fit models of DNA substitution[44,45] for each partition as suggested by the Akaike information criterion (Extended Data Table 1). Given that the Γ distribution accounts for rate heterogeneity, we did not include a proportion of invariant sites as recommended in ref. 46. If the model suggested by jModelTest was not implemented in RAxML 7.2.7 (ref. 29), we used the next most complex model. The 22-partition maximum likelihood analysis used RAxML 7.2.7 (ref. 29) (Extended Data Table 1; Supplementary Figs 1 and 2). RAxML analyses started from randomized maximum parsimony starting trees and employed the GTRCAT model with 500 bootstrap pseudoreplicates, and the fast hill-climbing algorithm. All other free parameters were estimated. Bootstrapping and a search for the maximum likelihood tree were performed in the same analysis (TreeBase submission number 15653).

Bayesian inference of correlated evolution. BayesTraits version 2.0 (software available from http://www.evolution.reading.ac.uk) was used to test for correlated evolution between the natural-log-transformed matrotrophy index and all other traits. The BayesTraits-Continuous module was used to compare two models of trait evolution: a dependent model in which two traits are assumed to evolve in a correlated fashion on the phylogeny, and an independent model in which the correlation between traits is set to zero using the *testcorrel* command. Three different sets of analyses were performed: the first set of analyses was run using the maximum likelihood phylogram from RAxML (Extended Data Table 2); the second was performed using ten trees sampled at regular intervals of 50 from the RAxML bootstrap analysis to control for phylogenetic uncertainty[48] (Extended Data Table 3); and the third was conducted using the maximum likelihood phylogram from RAxML and an imputed data set for all 177 poeciliid taxa in our phylogeny to evaluate the potential influence of missing values (Extended Data Table 4). The imputed data set was obtained using the phylogenetic data imputation technique implemented in PhyloPars[49], a web-based program that uses a maximum likelihood based method for estimating missing values assuming a Brownian motion model of trait evolution. The BayesTraits-Continuous module treats binary traits as continuous variables (BayesTraits does not allow mixture of continuous and binary variables, but see phylogenetic logistic regression below). If a binary trait is significantly correlated with the natural-log-transformed matrotrophy index (a quantitative variable), then the mean matrotrophy index for the group coded as zero differs significantly from the mean of the group coded as 1 (ref. 48). Average trait values were calculated for species with data from multiple populations and used in the analyses. Markov chain Monte Carlo analyses were run for 5,050,000 generations sampled every 1,000th iteration, with a burn-in of 50,000. The acceptance values of the transition rate parameter (*ratedev*) were within the required 20–40% for all analyses, ensuring adequate mixing among chains[48]. The scaling parameter lambda (λ) was simultaneously estimated to assess the contribution of the phylogeny to trait evolution ($\lambda = 0$ indicates phylogenetic independence and $\lambda = 1$ indicates phylogenetic dependence[47,48]). Best-fit models of trait evolution were selected by appraisal of the log(Bayes factors)[48,50], calculated as follows: log(Bayes factor) = 2(log[harmonic mean(dependent model)] − log[harmonic mean(independent model)]). On the log-scale, negative log(Bayes factors) argue in favour of the independent model of evolution; positive values support a dependent model of evolution, with log(Bayes factors) greater than 2 offering positive evidence and values greater than 5 strong evidence in favour of the dependent model[48].

Phylogenetic logistic regression. Phylogenetic logistic regressions (with Firth correction) were performed using PLogReg.m version 18Aug10 (ref. 51) in Matlab (Mathworks). The phylogeny was first exported from Mesquite version 2.75 (ref. 52) as a PDI file and converted to a phylogenetic variance–covariance matrix using the DOS program PDDIST[53] (available from the PDAP package in Mesquite). Sexual dimorphic coloration (dichromatism), courtship behaviour, exaggerated display traits and superfetation are binary traits. Their presence within each species was categorized as 1 and their absence as 0. The independent variable (the natural-log-transformed matrotrophy index) was standardized to have mean equal to 0 and

standard deviation equal to 1, so that the regression coefficients represented effect sizes of the independent variable whose magnitudes reflected the size of effect of the variable[51]. A bootstrapping procedure with 2,000 simulations was used to generate the confidence intervals and test for statistical significance of the slope of the regression model. Convergence of model parameters was achieved in all cases (Extended Data Table 5).

Phylogenetic generalized least-squares regression. Regressionv2.m version 16Mar11 (ref. 54) was used to assess linear relationships between the natural-log-transformed matrotrophy index and the sexual selection index, relative gonopodium length, sexual size dimorphism and $\log_{10}$-transformed male and female standard lengths and body weights. Mesquite version 2.75 (ref. 52) was employed to add populations as soft polytomies to the phylogeny. Population branch lengths were set at 0.0025 based on the mean of all population branch lengths in the original maximum likelihood phylogram, with the constraint that the tips of the population branches had to be lined up with the tip of the original species branch in the phylogeny. The MODEL procedure in SAS version 9.2 (SAS Institute) was used before all regressions to confirm a constant variance of residuals (homoscedasticity) by means of White's general and Breusch–Pagan tests (Extended Data Table 6; SAS/ETS 12.1 User's Guide[55]). Three regression models were then computed: (1) ordinary linear least-squares regressions assuming a star phylogeny; (2) phylogenetic generalized least-squares regressions assuming a Brownian motion process of trait evolution; and (3) phylogenetic generalized least-squares regressions assuming an Ornstein–Uhlenbeck process of trait evolution, which incorporates stabilizing selection towards an optimum value with different possible means for different groups. Ornstein–Uhlenbeck regression allows branch lengths to vary, estimating the optimal Ornstein–Uhlenbeck transformation parameter, d, with a value of 0 indicating that a star phylogeny (ordinary linear least-squares model) best fits the data, a value of 1 that the original input tree (phylogenetic generalized least-squares model) best fits the data and a value between 0 and 1 that 'intermediate branch lengths' provide the best fit[54]. For all statistical analyses, body weight and standard length were $\log_{10}$ transformed. To allow for soft polytomies, the degrees of freedom was corrected, using an adjusted degrees of freedom when comparing test statistics with critical F values of the total number of branches (N) – ($z + 2$), where z is the number of branches that are set to a length of zero[56,57]. Two approaches were used to select the best-fit linear regression model. First, we assessed differences in the Akaike information criterion (AIC): AIC = ($-2 \times \ln$(ML likelihood)) + ($2 \times$ number of parameters) between models, expressed as $\Delta_i = \mathrm{AIC}_i - \mathrm{AIC}_{\min}$ (where $\mathrm{AIC}_{\min}$ is the value of the model with the lowest AIC value and AIC_i is the value for the alternative model i). Δ_i provides a heuristic measure of the fit of alternative model i relative to the fit of the best model: $\Delta_i < 2$ suggests that there is substantial support for alternative model i relative to the best model; $4 < \Delta_i < 7$ indicates that the alternative model has considerably less support; and $\Delta_i > 10$ signifies that the alternative model is highly unlikely[58]. Second, where one model was a nested subset of the other (compared with the ordinary linear least-squares and phylogenetic generalized least-squares models, the Ornstein–Uhlenbeck model contains one more estimated parameter), we compared them by maximum likelihood ratio tests, where twice the difference in natural-log likelihoods between models ($D = -2$(maximum likelihood for best model − maximum likelihood for alternative model i)) is assumed to be distributed asymptotically as a χ^2 distribution with degrees of freedom equal to the difference in the number of parameters in the two models. Following ref. 54, we also used likelihood ratio tests to compare the phylogenetic generalized least-squares and ordinary linear least-squares models. Although the degrees of freedom in these comparisons is zero (both models have the same number of parameters), a difference in likelihoods greater than 3.841 (which is the ninety-fifth percentile of the distribution of χ^2 with one degree of freedom) is often taken to indicate a significant difference ($P > 0.05$) in the fit of the two models[54,59] (Supplementary Table 6).

31. Lovich, J. E. & Gibbons, J. W. A review of techniques for quantifying sexual size dimorphism. *Growth Dev. Aging* **56,** 269–281 (1992).
32. Fairbairn, D. J., Blanckenhorn, W. U. & Székely, T. (eds) *Sex, Size and Gender Roles: Evolutionary Studies of Sexual Size Dimorphism* (Oxford Univ. Press, 2007).
33. Meyer, A. & Lydeard, C. The evolution of copulatory organs, internal fertilization, placentae and viviparity in killifishes (Cyprinodontiformes) inferred from a DNA phylogeny of the tyrosine kinase gene *X-src*. *Proc. R. Soc. Lond. B* **254,** 153–162 (1993).
34. Meredith, R. W., Pires, M. N., Reznick, D. N. & Springer, M. S. Molecular phylogenetic relationships and the evolution of the placenta in *Poecilia* (*Micropoecilia*) (Poeciliidae: Cyprinodontiformes). *Mol. Phylogenet. Evol.* **55,** 631–639 (2010).
35. Meredith, R. W., Pires, M. N., Reznick, D. N. & Springer, M. S. Molecular phylogenetic relationships and the coevolution of placentotrophy and superfetation in *Poecilia* (Poeciliidae: Cyprinodontiformes). *Mol. Phylogenet. Evol.* **59,** 148–157 (2011).
36. Li, C., Ortí, G., Zhang, G. & Lu, G. A practical approach to phylogenomics: the phylogeny of ray-finned fish (Actinopterygii) as a case study. *BMC Evol. Biol.* **7,** 44 (2007).
37. Chen, W. J., Bonillo, C. & Lecointre, G. Repeatability of clades as a criterion of reliability: a case study for molecular phylogeny of Acanthomorpha (Teleostei) with larger number of taxa. *Mol. Phylogenet. Evol.* **26,** 262–288 (2003).
38. Hrbek, T., Seckinger, J. & Meyer, A. A phylogenetic and biogeographic perspective on the evolution of poeciliid fishes. *Mol. Phylogenet. Evol.* **43,** 986–998 (2007).
39. Kocher, T. D., Conroy, J. A., McKaye, K. R., Stauffer, J. R. & Lockwood, S. F. Evolution of NADH dehydrogenase subunit 2 in East African cichlid fish. *Mol. Phylogenet. Evol.* **4,** 420–432 (1995).
40. Ptacek, M. B. & Breden, F. Phylogenetic relationships among the mollies (Poeciliidae: *Poecilia*: *Mollienesia* group) based on mitochondrial DNA sequences. *J. Fish Biol.* **53** (Suppl. A), 64–81 (1998).
41. Breden, F., Ptacek, M. B., Rashed, M., Taphorn, D. & Figueiredo, C. A. Molecular phylogeny of the live-bearing fish genus *Poecilia* (Cyprinodontiformes: Poeciliidae). *Mol. Phylogenet. Evol.* **12,** 95–104 (1999).
42. Schmidt, T. R., Bielawski, J. P. & Gold, J. R. Molecular phylogenetics and evolution of the cytochrome *b* gene in the cyprinid genus *Lythrurus*. *Copeia* **1998,** 14–22 (1998).
43. Rambaut, A. Se-Al: Sequence Alignment Editor v.2.0a11 (http://tree.bio.ed.ac.uk/software/sea1, 1996).
44. Guindon, S. & Gascuel, O. A simple, fast, and accurate algorithm to estimate large phylogenies by maximum likelihood. *Syst. Biol.* **52,** 696–704 (2003).
45. Posada, D. jModelTest: phylogenetic model averaging. *Mol. Biol. Evol.* **25,** 1253–1256 (2008).
46. Yang, Z. *Computational Molecular Evolution* (Oxford Univ. Press, 2006).
47. Pagel, M. Inferring the historical patterns of biological evolution. *Nature* **401,** 877–884 (1999).
48. Pagel, M. & Meade, A. *User's Manual for BayesTraits V2* (http://www.evolution.rdg.ac.uk/Files/BayesTraitsV2Manual%28Beta%29.pdf, 2013).
49. Bruggeman, J., Heringa, J. & Brandt, B. W. PhyloPars: estimation of missing parameter values using phylogeny. *Nucleic Acids Res.* **37,** W179–W184 (2009).
50. Kass, R. E. & Raftery, A. E. Bayes factors. *J. Am. Stat. Assoc.* **90,** 773–795 (1995).
51. Ives, A. R. & Garland, T. Jr. Phylogenetic logistic regression for binary dependent variables. *Syst. Biol.* **59,** 9–26 (2010).
52. Maddison, W. P. & Maddison, D. R. Mesquite: A Modular System forEvolutionary Analysis v.2.75 (http://mesquiteproject.org, 2011).
53. Garland, T. Jr, Dickerman, A. W., Janis, C. M. & Jones, J. A. Phylogenetic analysis of covariance by computer simulation. *Syst. Biol.* **42,** 265–292 (1993).
54. Lavin, S. R., Karasov, W. H., Ives, A. R., Middleton, K. M. & Garland, T. Jr. Morphometrics of the avian small intestine compared with that of nonflying mammals: a phylogenetic approach. *Physiol. Biochem. Zool.* **81,** 526–550 (2008).
55. SAS Institute. *SAS/ETS 12.1 User's Guide* 1121–1122 (SAS Institute, 2012).
56. Purvis, A. & Garland, T. Jr. Polytomies in comparative analyses of continuous characters. *Syst. Biol.* **42,** 569–575 (1993).
57. Garland, T. Jr & Díaz-Uriarte, R. Polytomies and phylogenetically independent contrasts: an examination of the bounded degrees of freedom approach. *Syst. Biol.* **48,** 547–558 (1999).
58. Burnham, K. P. & Anderson, D. R. *Model Selection and Multimodel Inference: A Practical Information-Theoretic Approach* 2nd edn, 70–71 (Springer, 2002).
59. Felsenstein, J. *Inferring Phylogenies* (Sinauer, 2004).

Extended Data Table 1 | Results of models of molecular evolution chosen by jModelltest

Gene Region	DNA
12S 5’ Prime End; tRNA Val; 16S 5’ Prime End; 16S 3’ Prime End; tRNA Leu	GTR+ Γ
Cytb; ND1; ND2; COI	GTR+ Γ
tbr1	TrN+ Γ
Ptr	GTR+ Γ
zic1	GTR+ Γ
Plagl2	GTR+ Γ
RyR3	GTR+ Γ
srbe	TVM+ Γ
D8	TPM2uf+ Γ
T36	GTR+ Γ
D2	GTR+ Γ
D29	TrNef+ Γ
CCND1	TPM1uf+ Γ
RAB27	HKY+ Γ
Beta actin	TPM1uf+ Γ
Glyt	TPM3uf+ Γ
X-src	TrN+ Γ
ENC1	GTR+ Γ
Rag1	TIM1ef+ Γ
Rh	TPM3uf+ Γ
SH3PX3	GTR+ Γ
myh6	TrN+ Γ

Extended Data Table 2 | Bayesian inference of correlated evolution between the natural-log-transformed matrotrophy index and other life-history traits within the family Poeciliidae

Life history trait	N_{taxa}	log harmonic mean dependent model*	log harmonic mean independent model†	log Bayes Factor
Dichromatism	94	-194.869	-197.725	5.712[c]
Courtship behavior	79	-168.683	-169.750	2.134[b]
Ornamental male display traits	94	-150.789	-150.065	-1.448[a]
Sexual selection index	79	-213.129	-214.479	2.700[b]
Superfetation	92	-85.479	-93.698	16.438[c]
Relative gonopodium length	91	25.241	22.536	5.410[c]
Size dimorphism index body weight	78	-270.551	-274.089	7.076[c]
Sexual size dimorphism body weight	78	-113.943	-118.418	8.950[c]
Log_{10} male body weight	83	-152.150	-154.173	4.046[b]
Log_{10} female body weight	78	-161.862	-161.938	0.152[a]
Size dimorphism index standard length	89	-122.821	-125.126	4.610[b]
Sexual size dimorphism standard length	89	-20.562	-22.703	4.282[b]
Log_{10} male standard length	91	-59.788	-61.018	2.460[b]
Log_{10} female standard length	89	-78.310	-76.899	-2.822[a]

*Dependent model: correlation is assumed; †Independent model: correlation is set to zero. No evidence[a], positive evidence[b] and strong evidence[c] for correlated evolution[55].

Extended Data Table 3 | Bayesian inference of correlated evolution between the natural-log-transformed matrotrophy index and other life-history traits within the family Poeciliidae using a subset of ten trees to control for phylogenetic uncertainty

Life history trait	N_{taxa}	log harmonic mean dependent model*	log harmonic mean independent model†	log Bayes Factor
Dichromatism	94	-195.375	-202.029	13.308[c]
Courtship behavior	79	-168.603	-170.322	3.438[b]
Ornamental male display traits	94	-145.954	-146.285	0.663[a]
Sexual selection index	79	-212.830	-213.990	2.320[b]
Superfetation	92	-84.088	-96.953	25.730[c]
Relative gonopodium length	91	24.977	22.870	4.214[b]
Size dimorphism index body weight	78	-269.967	-273.299	6.664[c]
Sexual size dimorphism body weight	78	-115.281	-119.092	7.622[c]
Log_{10} male body weight	83	-152.985	-154.823	3.676[b]
Log_{10} female body weight	78	-161.153	-161.214	0.122[a]
Size dimorphism index standard length	89	-122.960	-125.434	4.948[b]
Sexual size dimorphism standard length	89	-20.190	-22.400	4.420[b]
Log_{10} male standard length	91	-60.527	-61.182	1.310[a]
Log_{10} female standard length	89	-76.677	-76.826	0.298[a]

*Dependent model: correlation is assumed; †Independent model: correlation is set to zero. No evidence[a], positive evidence[b] and strong evidence[c] for correlated evolution[55].

Extended Data Table 4 | Bayesian inference of correlated evolution between the natural-log-transformed matrotrophy index and other life-history traits after data imputation with PhyloPars

Life history trait	PhyloPars data set* (N_{taxa}=177)	$N_{imputed\_taxa}$	$\%_{imputed\_taxa}$	log harmonic mean dependent model	log harmonic mean independent model	log Bayes Factor
Dichromatism	1†§	83	46.89	-211.464	-214.952	6.976
	1†¶	83	46.89	-234.083	-236.996	5.826
	2‡§	83	46.89	-211.248	-215.160	7.824
	2‡¶	83	46.89	-233.356	-237.051	7.390
Courtship behaviour	1†§	98	55.37	-192.753	-192.774	0.042
	1†¶	98	55.37	-207.041	-207.832	1.582
	2‡§	98	55.37	-194.552	-195.221	1.338
	2‡¶	98	55.37	-207.052	-208.047	1.990
Ornamental male display traits	1†§	83	46.89	-93.501	-92.901	-1.200
	1†¶	83	46.89	-113.315	-113.147	-0.336
	2‡§	83	46.89	-92.892	-92.884	-0.016
	2‡¶	83	46.89	-112.383	-111.820	-1.126
Sexual selection index	1†§	98	55.37	-287.582	-288.485	1.806
	1†¶	98	55.37	-296.858	-297.374	1.032
	2‡§	98	55.37	-299.675	-300.724	2.098
	2‡¶	98	55.37	-315.085	-316.164	2.158
Superfetation	1†§	85	48.02	34.479	18.818	31.322
	1†¶	85	48.02	20.440	5.566	29.748
	2‡§	85	48.02	33.842	17.441	32.802
	2‡¶	85	48.02	19.770	5.592	28.356
Relative gonopodium length	1†	86	48.59	261.489	260.072	2.834
	2‡	86	48.59	262.196	260.886	2.620
Size dimorphism index body weight	1†	99	55.93	-371.865	-373.693	3.656
	2‡	99	55.93	-381.858	-384.999	6.282
Sexual size dimorphism body weight	1†	99	55.93	-19.479	-20.793	2.628
	2‡	99	55.93	-32.578	-36.179	7.202
Log_{10} male body weight	1†	94	53.11	-57.651	-60.727	6.152
	2‡	94	53.11	-63.672	-64.309	1.274
Log_{10} female body weight	1†	99	55.93	-42.388	-41.338	-2.100
	2‡	99	55.93	-51.771	-51.054	-1.434
Size dimorphism index standard length	1†	88	49.72	-37.529	-38.550	2.042
	2‡	88	49.72	-37.779	-40.491	5.424
Sexual size dimorphism standard length	1†	88	49.72	166.884	165.203	3.362
	2‡	88	49.72	165.629	163.514	4.230
Log_{10} male standard length	1†	86	48.59	96.946	96.064	1.764
	2‡	86	48.59	97.396	96.619	1.554
Log_{10} female standard length	1†	88	49.72	58.561	59.947	-2.772
	2‡	88	49.72	58.682	58.096	1.172

*Imputed data sets obtained with PhyloPars[55]; †Data set 1 (PhyloPars settings: correlated evolution of the different features is not allowed); ‡Data set 2 (PhyloPars settings: correlated evolution of the different features is allowed). For discrete traits we performed two separate analyses on each data set, using §raw (continuous) PhyloPars output values and ¶values rounded to the nearest integer, respectively.

Extended Data Table 5 | Ordinary and phylogenetic logistic regression parameter estimates for the effect of the natural-log-transformed matrotrophy index on dichromatism, courtship behaviour, ornamental male display traits and superfetation within the family Poeciliidae

Parameter	Estimate†	SE†	Bootstrap mean‡	Bootstrap 95%CI‡	Bootstrap *P*-value‡
Dichromatism					
Ordinary logistic regression					
b_0 (intercept)	0.263	0.226	0.235	(-0.288, 0.681)	0.322
b_1 (lnMI)	-0.822	0.301	-0.933	(-1.955, -0.374)	< 0.001
Ordinary logistic regression with Firth correction					
b_0 (intercept)	0.281	0.221	0.281	(-0.183, 0.733)	0.222
b_1 (lnMI)	-0.746	0.277	-0.756	(-1.509, -0.296)	< 0.001
Phylogenetic logistic regression with Firth correction*					
a	-1.576		-3.125	(-4.000, -1.917)	0.205
b_0	-0.099	0.343	-0.098	(-0.570, 0.367)	0.676
b_1 (lnMI)	-0.614	0.290	-0.626	(-1.360, -0.149)	0.007
Courtship behavior					
Ordinary logistic regression					
b_0 (intercept)	-0.247	0.279	-0.347	(-1.178, 0.249)	0.308
b_1 (lnMI)	-1.152	0.501	-1.444	(-3.541, -0.529)	< 0.001
Ordinary logistic regression with Firth correction					
b_0 (intercept)	-0.177	0.258	-0.178	(-0.814, 0.331)	0.522
b_1 (lnMI)	-0.953	0.425	-0.982	(-2.461, -0.346)	< 0.001
Phylogenetic logistic regression with Firth correction*					
a	-2.383		-3.146	(-4.000, -1.863)	0.236
b_0	-0.350	0.283	-0.349	(-0.949, 0.163)	0.181
b_1 (lnMI)	-0.763	0.380	-0.772	(-1.895, 0.187)	0.007
Ornamental male display traits					
Ordinary logistic regression					
b_0 (intercept)	-2.404	0.686	-2.709	(-4.623, -1.691)	< 0.001
b_1 (lnMI)	-2.087	1.467	-2.671	(-6.463, -0.742)	< 0.001
Ordinary logistic regression with Firth correction					
b_0 (intercept)	-1.903	0.451	-1.909	(-3.444, -1.280)	< 0.001
b_1 (lnMI)	-0.985	0.975	-0.987	(-4.157, -0.078)	0.023
Phylogenetic logistic regression with Firth correction*					
a	-1.840		-2.559	(-4.000, 1.147)	0.212
b_0	-2.387	0.529	-2.192	(-3.136, -0.720)	0.007
b_1 (lnMI)	-0.413	0.570	-0.361	(-2.095, 0.332)	0.429
Superfetation					
Ordinary logistic regression					
b_0 (intercept)	-1.061	0.278	-1.038	(-1.611, -0.459)	0.002
b_1 (lnMI)	1.314	0.362	1.462	(0.789, 2.659)	< 0.001
Ordinary logistic regression with Firth correction					
b_0 (intercept)	-1.066	0.271	-1.058	(-1.584, -0.545)	< 0.001
b_1 (lnMI)	1.204	0.332	1.204	(0.663, 2.083)	< 0.001
Phylogenetic logistic regression with Firth correction*					
a	1.293		-3.147	(-4.000, -1.922)	0.228
b_0	0.211	1.148	0.220	(-0.251, 0.708)	0.380
b_1 (lnMI)	0.776	0.301	0.788	(0.259, 1.760)	< 0.001

* Recommended models[36].
† Parameters of logistic regression and standard errors of the estimates were obtained using the GEE approximation[36].
‡ Parametric bootstrapping was performed by simulating 2000 data sets to obtain confidence intervals.

Extended Data Table 6 | White's general and Breusch–Pagan tests for homoscedasticity

	White's General test			Breusch-Pagan test		
Life history trait	Chi-sq.	*df*	*P*	Chi-sq.	*df*	*P*
Relative gonopodium length	4.21	4	0.3788	4.10	2	0.1289
Size dimorphism index body weight	0.74	4	0.9461	0.62	2	0.7342
Sexual size dimorphism body weight	2.38	4	0.6654	1.98	2	0.3715
Log_{10} male body weight	7.09	4	0.1314	5.70	2	0.0579
Log_{10} female body weight	5.52	4	0.2378	4.46	2	0.1077
Size dimorphism index standard length	1.47	4	0.8314	0.30	2	0.8613
Sexual size dimorphism standard length	1.47	4	0.8320	0.72	2	0.6975
Log_{10} male standard length	6.97	4	0.1373	6.09	2	0.0476
Log_{10} female standard length	5.82	4	0.2128	5.33	2	0.0697